Synthesis, Crystal Structure, and Electrochemistry of Mono- and Bis-Homoannular Ferrocene Derivatives

Uttam R. Pokharel [1],* Derek Daigle [1], Stone Naquin [1], Gwyneth Engeron [1], Mary Lo [1] and Frank R. Fronczek [2]

[1] Nicholls State University, Thibodaux, Louisiana 70301, USA

[2] Louisiana State University, Baton Rouge, Louisiana 70803, USA

* Correspondence: uttam.pokharel@nicholls.edu

Abstract: Two ferrocene derivatives, namely, 1,2-(tetramethylene)-ferrocene and 1,2,1′,2′-bis(tetramethylene)-ferrocene, were synthesized in a four-step reaction sequence starting from ferrocene. Friedel-Craft acylation of ferrocene with succinic anhydride gave mono- or bis(3-carboxypropinoyl)ferrocene depending on the stoichiometry of succinic anhydride. The reduction of the keto groups to methylene, followed by ring-closing using trifluoroacetic anhydride gave 1,2-(α-ketotetramethylene)-ferrocene or 1,2,1′,2′-bis(α-ketotetramethylene)ferrocene. The diastereomeric mixture of the latter diketones was separated by column chromatography, characterized by single-crystal X-ray analysis, and assigned their stereochemistry. Reduction of the keto groups to methylene under Clemmensen conditions gave homoannular mono- or bis(tetramethylene) ferrocene derivatives. The molecular structure of 1,2-(tetramethylene)-ferrocene revealed that the *ipso* carbon atoms of the cyclopentadienyl group are 0.023(3) Å farther away from Fe(II) compared to the remaining three carbon atoms. Both complexes exhibit lower half-wave oxidation potentials than ferrocene, possibly due to the electron-releasing effects of the tetramethylene bridges.

Keywords: 1,2-(α-ketotetramethylene)-ferrocene; 1,2-(tetramethylene)-ferrocene; ferrocene; Friedel-Crafts acylation; Clemmensen reduction; X-ray crystallography; planar chirality; puckering parameters; electrochemistry

1. Introduction

Ferrocene and its derivatives play important roles in modern-day materials chemistry owing to their air stability, aromatic reactivity, reversible electrochemistry, and low toxicity [1]. Ferrocene, since its discovery in 1951 [2], has been considered an analog of benzene for its aromatic properties. Benzene has been homologated up to 13 linearly fused rings [3], and the higher polycyclic aromatic hydrocarbons are promising candidates for organic optoelectronic applications [4]. However, the benzannulation of ferrocene to extend the π-conjugation of its cyclopentadienide (Cp⁻) ring is limited to indenide (Ind⁻) [5–8]. The indenide complexes of iron are commonly synthesized by direct metallation of the conjugate base of indene with Fe(II) synthons [9,10]. This method has limitations associated with the inherent synthetic difficulties of ligands for higher benzannulated ferrocene derivatives.

With our continuous interests in extending the π-conjugation of metallocenes [11], we synthesized 1′,2′,3′,4′,5′-pentamethylruthenocene-fused quinones from the double Friedel-Crafts acylation between metallocene-1,2-diacylchloride and organic aromatics [12]. Our attempts to reductively aromatize quinones were not successful. Later, we realized that switching the functionality of two reaction partners can give such complexes by a much simpler method. Ferrocene being an excellent nucleophile for Friedel-Crafts reactions, its reaction with succinic anhydride can eventually lead us to the conjugation of tetramethylene groups to one or both of its cyclopentadienyl rings [13]. These compounds can serve as the simplest possible precursors for extending the π-

conjugation in ferrocene by dehydrogenation. In this contribution, we report the synthesis of 1,2-(tetramethylene)-ferrocene and 1,2,1′,2′-bis(tetramethylene)-ferrocene starting from ferrocene, molecular structures of key synthetic products, and the half-wave oxidation potentials of the final products.

2. Materials and Methods

2.1. General Procedures

Reactions were carried out using standard Schlenk line techniques under nitrogen unless otherwise described. Reagent grade solvents and chemicals were purchased and used as received. Ferrocene, succinic anhydride, aluminum chloride, zinc powder, mercuric chloride (Alfa Aesar), and trifluoroacetic anhydride (Oakwood Chemicals) were used as purchased.

^{1}H and ^{13}C NMR spectra were recorded on a JEOL – 400 ESZ spectrometer at room temperature and were referenced to residual solvent peaks. Infrared spectra were recorded on a Bruker Alpha-E FT-IR spectrometer with a diamond crystal ATR accessory. Melting points were taken on a Thomas-Hoover capillary melting point apparatus and were uncorrected. Half-wave oxidation potentials were determined using a BASi Epsilon – Electrochemical Workstation.

2.2. X-ray Crystallography

X-ray diffraction data were measured at T = 90 K on a Bruker Kappa Apex-II diffractometer equipped with a sealed-tube MoKα source (λ=0.71073 Å), a Triumph focusing monochromator and a CCD detector. Structures were solved using SHELXT [14] and refined using SHELXL [15]. Hydrogen atoms were visible in difference maps and were placed in idealized positions during refinement and treated as riding. The structure of **3b′** had a disorder involving partially occupied carbonyl groups at CH$_2$ sites. The crystal structures and refinement data are presented in Table 1.

2.3. Experimental Procedures

1-(3-Carboxypropionyl)ferrocene (1a). To a stirred solution of ferrocene (3.02 g, 16.3 mmol) in dichloroethane (40 mL), a suspension of succinic anhydride (1.83 g, 18.1 mmol) and aluminum chloride (4.20 g, 32.1 mmol) in dichloroethane (80 mL) was slowly added over a 45-min period. The reaction mixture was stirred for an additional 2 h at room temperature, then poured into ice-cold water (50 mL). The organic phase was extracted in dichloromethane (3 x 50 mL). The product was again extracted in 1.0 M NaOH (3 x 20 mL), and the aqueous layer was neutralized with concentrated HCl. The precipitate was collected by filtration, washed with water, and dried to give **1a** (1.78 g, 38%) as an orange powder. Melting point: 165–166 °C (Lit. [16] 164 – 165). **^{1}H NMR (400 MHz, CDCl$_3$):** δ 2.72 – 2.76 (t, 2 H, ^3J = 6.8 Hz), 3.06 – 3.09 (t, 2 H, ^3J = 6.4 Hz), 4.23 (s, 5 H, Cp), 4.51 – 4.52 (t, 2 H, ^3J = 2.4 Hz), 4.80 – 4.81 (t, 2 H, ^{3}J = 2.0 Hz). **IR**: 1705 cm^{-1} (carboxylic C=O), 1657 cm^{-1} (ketonic C=O).

1,1′-Bis(3-carboxypropionyl)ferrocene (1b). To a suspension of succinic anhydride (10.8 g, 108 mmol) and anhydrous aluminum chloride (28.8 g, 216 mmol) in dichloroethane (80 mL), a solution of ferrocene (10.0 g, 53.8 mmol) in dichloroethane (80 mL) was added slowly. The reaction was stirred for 48 h at room temperature and poured into ice-cold water (100 mL). The organic phase was collected and the aqueous phase was extracted with dichloromethane (2 x 100 mL). The product was extracted from the organic phase with 2 M sodium hydroxide (3 x 100 mL). The aqueous phase was neutralized with conc. HCl. The precipitate was collected by filtration. The crude product was suspended in boiling water (100 mL) and filtered to give **1b** (14.9 g, 72%) as a dark red powder. Melting Point: 178 – 179 °C (Lit. [17] 179 °C). **^{1}H NMR (400 MHz, acetone-d$_6$, ppm):** δ 2.60 – 2.64 (t, 4 H, ^3J = 6.4 Hz), 3.02 – 3.05 (t, 4H, ^3J = 6 Hz), 4.62 – 4.63 (t, 4H, ^3J = 3.6 Hz), 4.89 – 4.90 (t, 4 H, ^3J = 2.4 Hz).

1-(3-carboxypropyl)ferrocene (2a). This compound was synthesized using procedures reported in the literature [18]. Yield: 54%. Melting Point: 115 – 116 °C (Lit. [16] 115 – 116 °C). **^{1}H NMR (400 MHz, CDCl$_3$, ppm):** δ 1.80 – 1.87 (m, 4 H), 2.35 – 2.40 (m, 8 H), 3.98 – 4.09 (m, 8 H).

1,1′-bis(3-carboxypropyl)ferrocene (2b). This compound was synthesized following procedures reported in the literature [17]. Yield: 90%. Melting Point: 72 – 73 °C (Lit. [17] 73 °C). **^{1}H NMR (400 MHz, CDCl$_3$, ppm):** δ 1.80 – 1.87 (m, 4H), 2.35 – 2.40 (m, 8H), 43.98 – 4.09 (m, 8H). **^{13}C{^{1}H} NMR (100 MHz, CDCl$_3$, ppm):** δ 25.95, 28.58, 33.64, 67.89, 68.88, 77.32, 88.08, 179.97. **IR**: 1703 cm^{-1} (C=O), 3000 – 3200 cm^{-1} (OH).

1,2-(α-ketotetramethylene)-ferrocene (3a). This compound was synthesized by following procedures in the literature [19]. Yield: 81%. Melting Point: 82 – 83 °C (Lit. [20] 83 – 85 °C) **^{1}H NMR (400 MHz, CDCl$_3$, ppm):** δ 2.02 – 2.22 (m, 2H), 2.25 – 2.45 (m, 2H), 2.59 – 2.67 (m, 2H), 4.17 (s, 5H, Cp), 4.45 – 4.47 (m, 2H, Cp), 4.81 – 4.82 (m, 1H, Cp). **^{13}C{^{1}H} NMR (100 MHz, acetone-d$_6$, ppm):** δ 23.4, 23.9, 38.8, 64.6, 70.0, 75.8, 92.5, 202.4. **IR**: 1664 cm^{-1} (C=O). The product was analyzed by single crystal X-ray analysis.

Isomeric 1,2,1′2′-bis(α-ketotetramethylene)-ferrocenes (3b and 3b′). To a stirred solution of **2b** (0.501 g, 1.40 mmol) in dichloromethane (15 mL), a solution of trifluoroacetic anhydride (0.778 mL, 5.59 mmol) in dichloromethane (15 mL) was added dropwise. The reaction was stirred for 20 h at room temperature. A saturated solution of sodium bicarbonate (100 mL) was added to the mixture. The organic phase was collected, and the aqueous phase was extracted with dichloromethane (50 mL). The organic phase was washed with water (2 × 20 mL), dried with magnesium sulfate, and filtered. The volatiles were removed *in vacuo* to give **3b** and **3b′** (0.190 g, 42%) as a bright red powder. The two diastereomers (**3b** and **3b′**) were separated by silica column chromatography using a mixture of ethyl acetate and dichloromethane (2:1) as eluent. The racemic mixture (dark red) **3b′,** was followed by the *meso* (dark orange), **3b**, in the column.

3b (*Meso):* Melting Point: 168 -189 °C (Lit. [21] 161 -167 °C. **^{1}H NMR (400 mHz, CDCl$_3$):** δ 2.00 - 2.11 (m, 4H, CH2), 2.15 – 2.40 (m, 6H, CH2), 2.56 – 2.66 (m 4H CH2), 4.42 – 4.45 (m, 2H, Cp), 4.73 (b, 2H, Cp). **^{13}C{^{1}H} NMR (100 MHz, CDCl$_3$, ppm):** δ 22.92, 23.66, 39.27, 67.38, 72.37, 73.19, 76.58, 93.42, 204.33. **IR**: 1661 cm^{-1} (C=O). The product was characterized by single crystal X-ray analysis.

3b′(*Racemic*)*:* Melting Point: 156 - 157 °C (Lit. [21] 153 – 161 °C). **^{1}H NMR (400 MHz, CDCl$_3$):** δ 2.01 – 2.15 (m, 2 H), 2.21 – 2.47 (m, 6H), 2.61 (dt, ^{2}J = 15.6 Hz, ^{3}J = 4.4 Hz, 4 H), 4.39 (d, ^{3}J = 1.2 Hz, 2H), 4.42 – 4.43 (m, 4 H), 4.65 (t, 3J = 1.2 Hz, 2 H). **^{13}C{^{1}H} NMR (100 MHz, CDCl$_3$, ppm):** δ 23.32, 23.52, 39.20, 68.03, 70.84, 71.85, 77.32, 94.00, 203.40 **IR**: 1663 cm^{-1} (C=O). The product was analyzed by single crystal X-ray analysis.

1,2-(tetramethylene)-ferrocene (4a) and 1,2,1′,2′-bis(tetramethylene)-ferrocene (4b). The experimental setup and procedure were the same as that for 2a.

4a. Yield: 87%. Melting point: 39 °C (Lit. [22] 39 – 41 °C) **^{1}H NMR (400 MHz, Acetone-d$_6$, ppm):** δ 1.53 – 1.64 (m, 2H), 1.85 – 1.92 (m, 2H), 2.17 – 2.26 (m, 2H), 2.60 – 2.67 (m, 2H), 3.85 (t, ^{3}J = 2.4 Hz, 1H, CHC*H*CH), 3.94 (d, ^{3}J = 2.4 Hz, 2H, C*H*CHC*H*), 3.95 (s, 5H, Cp). **^{13}C{^{1}H} NMR (100 MHz, acetone-d$_6$, ppm):** δ 23.5, 24.6, 64.8, 65.1, 69.4, 84.9.

4b. Yield**:** 59%. **^{1}H NMR (400 MHz, acetone-d$_6$):** δ 1.53 – 1.57 (m, 4H), 1.85 – 1.88 (m, 4H), 2.16 – 2.23 (m, 4H), 2.57 – 2.64 (m, 4H), 3.65 (t, ^{3}J = 2.4 Hz, 2H, CHC*H*CH), 3.76 (d, 3J = 2.4 Hz, 4H, C*H*CHC*H*). **^{13}C{^{1}H} NMR (100 MHz, acetone-d$_6$, ppm):** δ 23.6, 23.9, 67.5, 68.3, 84.2.

3. Results and discussion

3.1. Synthesis and Structural Elucidation of Compounds 1a, 1b – 4a, 4b

Synthesis of the target compounds (**4a** and **4b**) was performed by following the reaction sequence as shown in Scheme 1. Our attempts to reproduce the procedures reported in the literature [23,24] resulted in the formation of an approximately equimolar mixture of mono-and bis(3-carboxypropenoyl)ferrocene. To avoid the tedious separation of these two keto-carboxylic acids, we synthesized (3-carboxypropenoyl)ferrocene, **1a** (38%) by slowly adding a suspension of succinic anhydride and aluminum chloride in dichloroethane to the solution of ferrocene in the same solvent. The procedure left some unreacted ferrocene, but the product was purified by solvent extraction using NaOH solution. Synthesis of bis(3-carboxypropenoyl)ferrocene, **1b** (72%) was performed by adding ferrocene into the suspension of succinic anhydride and aluminum chloride and stirring the

solution at room temperature for 48 h. After the base extraction, the product was found to contain **1a** as an impurity, which was removed by washing with boiling water. The Clemmensen reduction of both keto carboxylic acids, **1a** and **1b**, was performed by following literature procedures [17,18] to give 1-(3-carboxypropyl)ferrocene, **2a** (54%) and 1,1′-bis(3-carboxypropyl)ferrocene, **2b** (90%) respectively.
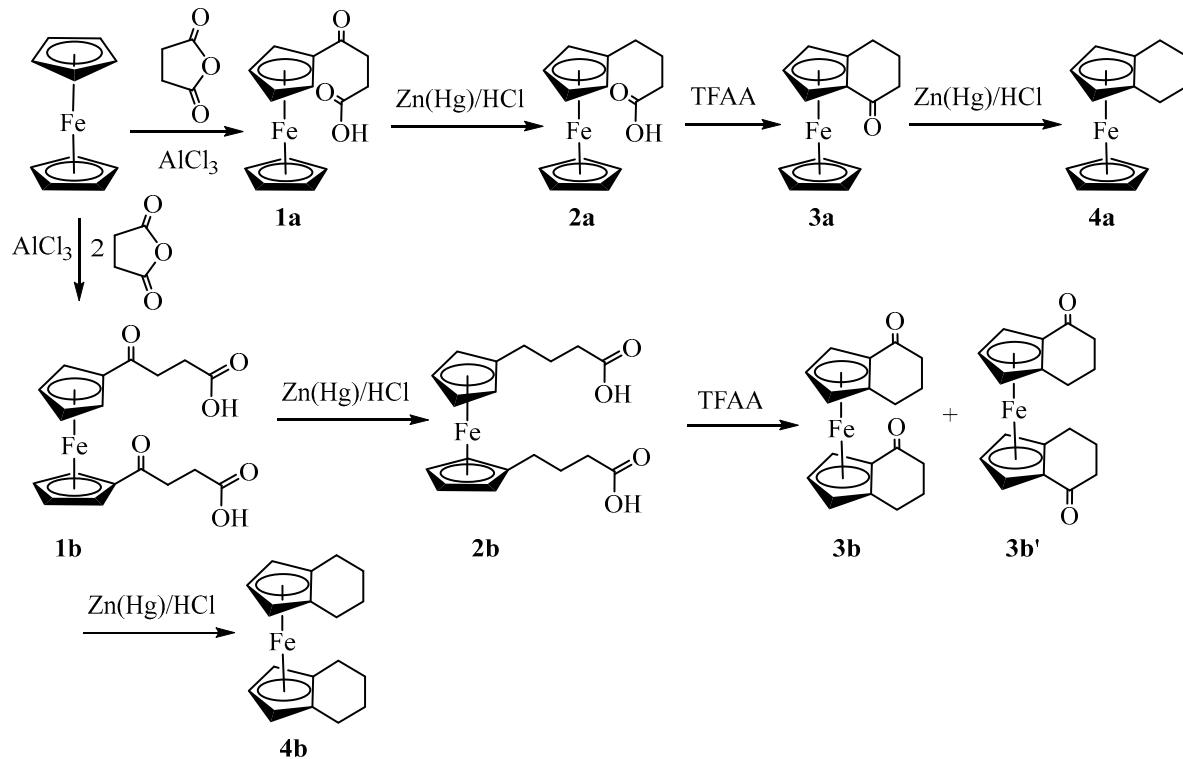
Scheme 1. Synthesis of homoannular ferrocene derivatives.

The ring closing of **2a** and **2b** was performed in the presence of trifluoroacetic anhydride [19,21] to give homoannularly cyclized products: 1,2(α-ketotetramethylene)ferrocene, **3a** (81%) and 1,2,1′,2′-bis(α-ketotetramethylene)ferrocene, **3b** (42%) respectively. The ^{1}H NMR analysis of the crude product **3b** revealed the formation of two geometric isomers (**3b** and **3b′**) in an approximately 1:1 ratio. The diastereomers were separated by column chromatography. Distinctive ABC patterns of substituted cyclopentadienyl rings in ^{1}H NMR for each compound indicated the formation of desired products. Similarly, the diastereotopic nature of *exo-* and *endo-*protons of the methylene groups exhibited a complex coupling pattern giving a set of multiplets (Figures S1, S4 and S7). Assignment of the stereochemistry of these geometrical isomers (*meso*, **3b** and *racemic*, **3b′**) was achieved by single crystal *X*-ray analysis (*vide infra*). Although Nesmeyanov [25] and Rinehart [13,21] independently reported the synthesis of **3a** and **3b**, their full characterization data were not available. The authors were unable to assign the configurations of the geometric isomers of **3b** [21].

Reductions of the carbonyl group of **3a** and **3b** to methylene were performed under Clemmensen conditions to give 1,2-(tetramethylene)-ferrocene **4a** (87%) and 1,2,1′,2′-bis(tetramethylene)-ferrocene **4b** (59%), respectively. The appearance of triplets (1H) and doublets (2H) on the substituted cyclopentadienyl rings in ^{1}H NMR indicated the formation of desired products. Like ketones (**3a**, **3b,** and **3b′**), the diastereotopic nature of the *exo-* and *endo-*hydrogens of the methylene group gave a complicated coupling pattern in ^{1}H NMR. Both signals of the cyclopentadienyl rings are shifted upfield for both **4a** and **4b** but the shift is more prominent for **4b** (triplet at 3.65 and doublet at 3.75 ppm) (Figures S10 and S12). Synthesis of compounds **4a** [22] and **4b** [26–28] were previously reported with limited characterization data. Our attempts to dehydrogenate **4a** and **4b** using 2,3-dichloro-5,6-dicyanoquinone (DDQ) resulted in the formation of intractable black products with limited solubility in organic solvents, possibly due to the formation of charge-transfer complexes [29].

3.2. X-ray Crystal Structures

The structures of ferrocene derivatives **3a**, **3b**, **3b'**, and **4a** were determined by X-ray crystallography. All crystals were grown by slow evaporation of concentrated ethyl ether solutions in air at room temperature. Thermal ellipsoid plots with numbering schemes are shown in Figures 1–4. The crystal and refinement data for these compounds are given in Table 1. The crystal structure of **3a** has been reported by Fleischer, et al. at room temperature [30]. We have redetermined its crystal structure at 90 K with much higher precision. The compound **3a** exhibits planar chirality since two different substituents are connected to the cyclopentadienyl ring [31]. As the compound crystallizes in centrosymmetric space group (P−1), the two enantiomers Rp/Sp are present equally in the crystals. The iron atom in compound **3b** lies on a crystallographic inversion center. Compound **3b'** crystallizes with Z' = 2 in which one of the molecules has a disorder of the O atom into two positions. The **3b'** crystallizes as a racemic mixture in a centrosymmetric space group $P2_1/n$. The two molecules have roughly perpendicular orientations. Each molecule possesses an approximate two-fold rotation axis (Figure 3). Compound **4a** crystallizes in the monoclinic space group $P2_1/c$ with one molecule per asymmetric unit.
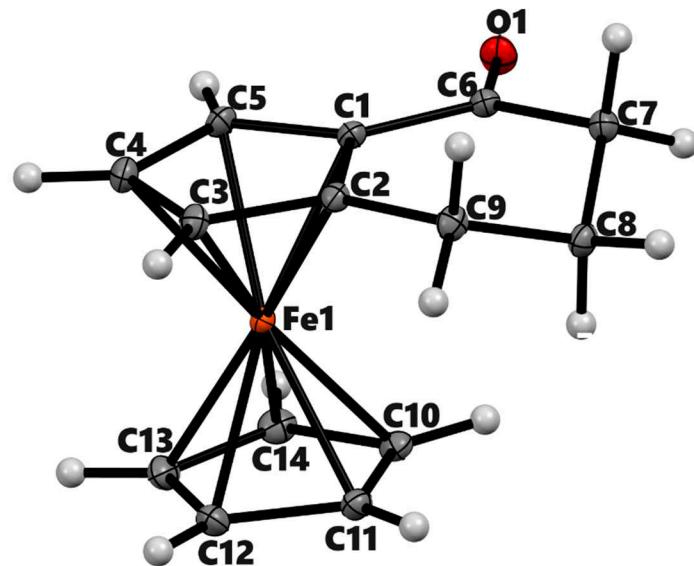
Figure 1. ORTEP diagram of solid-state structure showing the atom-numbering scheme of compound **3a.** Thermal ellipsoids are drawn at the 50% probability level. Selected bond lengths (Å) for the complex: Fe1–C1 2.0397(9), Fe1–C2 2.0508(8), Fe1–C3 2.0526(6), Fe1–C4 2.0527(7), Fe1–C5 2.0456(9), Fe1–C10 2.0553(7), Fe1–C11 2.0530(8), Fe1–C12 2.045(1), Fe1–C13 2.0548(9), Fe1–C14 2.0554(6), C1–C6 1.465(1), C6–O1 1.2265(9), Cp (centroid, substituted) – Fe 1.647, Cp (centroid, unsubstituted) 1.655.

In the molecules **3a**, **3b,** and **3b',** the ferrocenyl moiety is fused with α-keto tetramethylene rings on one or both cyclopentadienyl rings, while in the molecule **4a**, the ferrocenyl moiety is fused with a tetramethylene ring. In all cases, the angle between Fe and two Cp ring centroids is nearly 180° with a maximum deviation of 4.85° from linear geometry in **3b'**. The Cp rings in the ferrocene system are almost parallel; as the dihedral angle between the planes of the two Cp rings in **3a**, **3b',** and **4a** are 1.84°, 3.46° (average of two), and 1.92°, respectively. The Cp rings display nearly eclipsed conformation in **3a**, **3b'**and **4a**, as demonstrated by C – Cg1 – Cg2 – C average torsion angles of 9.12°, 0.26°, and 6.12° respectively. The Cp rings in **3b** are perfectly staggered (torsional angles 36.00°) as required by the inversion center located at Fe.
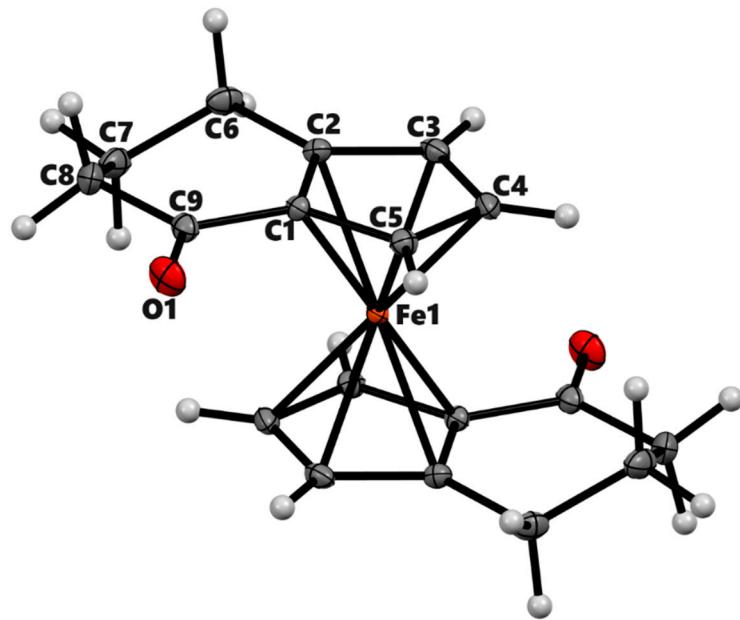
Figure 2. ORTEP diagram of the solid-state structure showing the atom-numbering scheme of compound **3b** (*meso*). Thermal ellipsoids are drawn at the 50% probability level. Selected bond lengths (Å) for the complex: Fe1–C1 2.0397(8), Fe1–C2 2.0627(7), Fe1–C3 2.0605(8), Fe1–C4 2.0664(8), Fe1–C5 2.0511(7), O1–C9 1.2230(9), Cp (centroid)–Fe 1.660.

Within the ferrocenyl moieties, the mean Fe – C bond distances for unsubstituted Cp are unremarkable. However, the Fe–C distance for the *ipso* carbon-bearing keto group next to it is slightly shorter than the rest of the distances. For instance, the Fe1 – C1 bond in compound **3a** is 2.0397(9) Å while the average distance of Fe1 with C2 to C5 is 2.0505(7) Å. The slippage of the Fe center towards C1 has been observed in other α-keto ferrocenyl derivatives [32,33]. It presumably occurs to maximize the interaction of the Fe center with the exocyclic double bond in the resonance of such ketones [34]. The attached carbonyl group lies almost co-planar with the substituted cyclopentadienyl ring in **3a** **3b** and **3b'** as given by the torsional angle [C5-C1-C6-O1 = 1.52(11)°] in **3a**. The C=O bond lengths in **3a** 1.2265(9) Å, **3b** 1.2230(9) Å, and **3b'** 1.225 (17) Å are in normal range of similar α-ferrocenyl ketones [35,36]. In **4a**, the average distance of Fe1-C1 and Fe1-C2 is higher by 0.023(3) Å than the rest of Fe-C bonds of the substituted cyclopentadienyl ring. The distance from the Fe center to the centroid of cyclopentadienyl rings ranges from 1.647 Å to 1.660 Å.
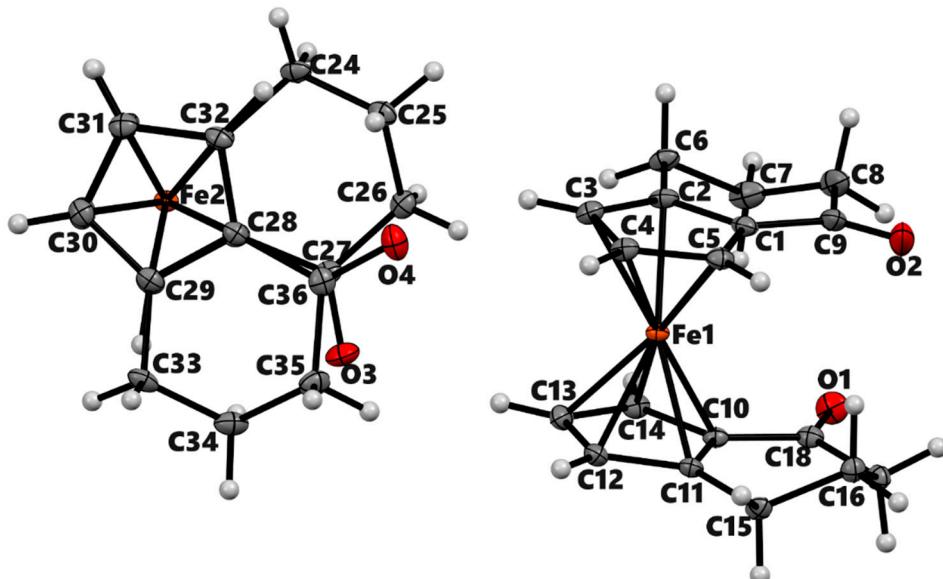
Figure 3. ORTEP diagram of the solid-state structure showing the atom-numbering scheme of compound **3b'**. Thermal ellipsoids are drawn at the 50% probability level. The minor component of disordered O-atom is not shown. Selected bond lengths (Å) for the complexes: Fe1–C1 2.0409(7), Fe1–C2 2.0575(7), Fe1–C3 2.0681(7), Fe1–C4 2.0534(7), Fe1–C5 2.0442(7), Fe1–C10 2.0469(6), Fe1–C11 2.0688(6), Fe1–C12 2.0615(7), Fe1–C13 2.0566(7), Fe1–C4 2.0534(7), Fe1–C4 2.0534(7), O2–C9 1.2212(17), average Cp(Centroid)–Fe 1.652.

The six-membered rings in all structures adopt half-chair conformations. The Cremer & People puckering parameters [37] of the six-membered rings, namely, **3a**, **3b**, **3b'** and **4a** are Q_T = 0.4340(8) Å, θ = 131.43(11)° and φ = 2.47(14)°; Q_T =0.4227(8) Å, θ = 129.68(10)° and φ = 358.42(13)°; Q_T = 0.4356(12) Å, θ = 53.54(14)° and φ = 178.20(18)°; and Q_T = 0.521(3) Å, θ = 51.7(3)° and φ = 219.0(4)°, respectively. In **3a**, atoms C6/C7/C9 lie on the same plane as the substituted cyclopentadienyl ring with a dihedral angle of 1.80°. The C8 projects inward from the main plane of Cp by 0.582 Å. Similar folding of six-membered rings can be seen in **3b** and **3b'** as well. The two α-ketotetramethylene groups are oriented with dihedral angles of 180° and 72° in **3b** and **3b'**, respectively. The six-membered ring of **4a** is more twisted than in **3a** or **3b**. In this molecule, **C6** and **C9** are almost coplanar with the substituted Cp [deviation: C6 = 0.018 Å, C9 = 0.033 Å]. The C7 is projected down by 0.498 Å and C8 is projected up by 0.305 Å from the Cp plane.
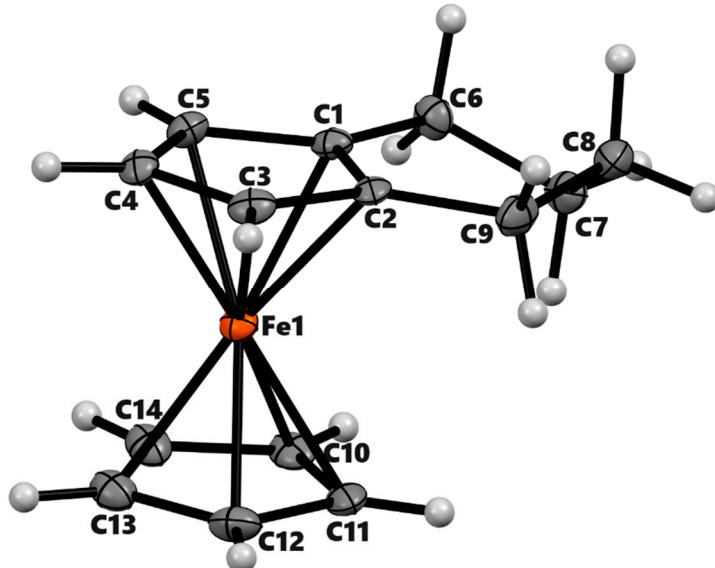
Figure 4. ORTEP diagram of the solid-state structure showing the atom-numbering scheme of compound **4a**. Thermal ellipsoids are drawn at the 50% probability level. Selected bond lengths (Å) for the complexes: Fe1–C1 2.049(3), Fe1–C2 2.064(3), Fe1–C3 2.040(3), Fe1–C4 2.034(2), Fe1–C5 2.031(3), Fe1–C10 2.043(3), Fe1–C11 2.036(3), Fe1–C12 2.045(3), Fe1–C13 2.051(3), Fe1–C14 2.042(3), Cp (centroid, substituted) – Fe 1.647, Cp (centroid, unsubstituted) 1.648.

Table 1. Crystal data and refinement parameters.

	3a	3b *(meso)*	3b' *(racemic)*	4a
Chemical formula	$C_{14}H_{14}FeO$	$C_{18}H_{18}FeO_2$	$C_{18}H_{18}FeO_2$	$C_{14}H_{16}Fe$
M_r	254.1	322.17	322.17	240.12
Deposition No.	CCDC 2322201	CCDC 2322202	CCDC 2322203	CCDC 2322204
Crystal system, space group	Triclinic, *P*-1	Monoclinic, *P*2₁/*n*	Monoclinic, *P*2₁/*n*	Monoclinic, *P*2₁/*c*
Temperature (K)	90	90	90	90
a, b, c (Å)	6.5983 (4), 7.7105 (4), 11.8843 (7)	7.422 (2), 7.551 (2), 12.366 (4)	13.6414 (6), 14.7516 (6), 13.8763 (6)	7.661 (3), 9.506 (4), 14.642 (6)

α, β, γ (°)	108.140 (3), 90.461 (3), 108.897 (3)	90, 100.397 (14), 90	90, 99.432 (2), 90	90, 95.574 (6), 90
V (Å^3)	539.61 (6)	681.6 (3)	2754.6 (2)	1061.4 (7)
Z	2	2	8	4
Radiation type	Mo $K\alpha$	Mo $K\alpha$	Mo $K\alpha$	Mo $K\alpha$
μ (mm^{-1})	1.37	1.11	1.10	1.38
Crystal size (mm)	0.16 × 0.15 × 0.06	0.36 × 0.20 × 0.11	0.44 × 0.39 × 0.36	0.15 × 0.11 × 0.06
Diffractometer	Bruker Kappa *APEX*-II DUO	Bruker Kappa *APEX*-II	Bruker Kappa *APEX*-II DUO	Bruker Kappa *APEX*-II DUO
Absorption correction	Multi-scan	Multi-scan	Multi-scan	Multi-scan
T_{min}, T_{max}	0.863, 0.922	0.750, 0.888	0.657, 0.749	0.753, 0.922
No. of measured, independent and observed [$I > 2\sigma(I)$] reflections	22162, 9304, 7739	22653, 5593, 4567	74998, 21250, 16339	16912, 3242, 1949
R_{int}	0.025	0.026	0.028	0.139
$(\sin \theta/\lambda)_{max}$ (Å^{-1})	1.042	1.018	0.974	0.716
$R[F^2 > 2\sigma(F^2)]$, $wR(F^2)$, S	0.034, 0.081, 1.04	0.030, 0.084, 1.07	0.033, 0.090, 1.05	0.052, 0.100, 1.00
No. of reflections	9304	5593	21250	3242
No. of parameters	187	97	400	136
No. of restraints	0	0	9	0
H-atom treatment	Only H-atom coordinates refined	H-atom parameters constrained	H-atom parameters constrained	H-atom parameters constrained
$\Delta\varrho_{max}$, $\Delta\varrho_{min}$ (e Å^{-3})	1.38, −0.75	1.05, −0.77	1.47, −0.53	0.66, −0.85

In their crystal structures, compounds **3a**, **3b,** and **3b'** display similar intermolecular interactions. The most prominent contacts are weak intermolecular C-H···O hydrogen bonds and C-H···π interactions. For example, molecules of **3b** exhibit intermolecular C-H4···O1, C-H5···O1 interactions along the crystallographic *b*-axis. Similarly, atom H8A is positioned almost perpendicularly above the cyclopentadienyl ring centroid of the adjacent molecule (Figure S14). In the crystal structure of **4a**, there are C-H···π interactions between methylene hydrogen and the cyclopentadienyl rings (Figure S15).

3.3. Electrochemical studies

To investigate the effects of tetramethylene substituents on the oxidation potential of the ferrocene moiety, we measured the half-wave redox potentials ($E_{1/2}$) of **4a** and **4b** by cyclic voltammetry using 0.1 M tetrabutylammonium hexafluorophosphate in dichloromethane as a supporting electrolyte at a scan rate of 50 mV s^{-1} in 10^{-3} M concentration. All measurements were carried out at room temperature under a dry nitrogen atmosphere by the use of a three-electrode system: glassy carbon as the working electrode, Ag/AgCl as the reference electrode, and platinum wire as a counter electrode.

Like ferrocene, the cyclic voltammetry of **4a** and **4b** shows a single-electron reversible redox process (Figure 5). As expected, the redox potentials of both complexes are lower than that of ferrocene due to the electron-donating ability of tetramethylene rings. The higher electron density at the iron center due to the tetramethylene ring causes the iron center to lose an electron more easily as compared to ferrocene [38]. Under the experimental conditions, the $E_{1/2}$ of ferrocene, **4a** and **4b** are 499 mV, 303 mV, and 183 mV, respectively *versus* Ag/Ag$^+$. Thus, the oxidation potential of **4a** is 196 mV lower than that of ferrocene. Addition of the second tetramethylene group, as in **4b**, lowers the

potential by 316 mV, nearly twice the value found between **4a** and ferrocene. A slight deviation of the values from linearity might be due to experimental errors. Similar additivity effects of substituents on the oxidation potential of ferrocene have been reported in ferrocene derivatives with increasing number of similar substituents [39,40].
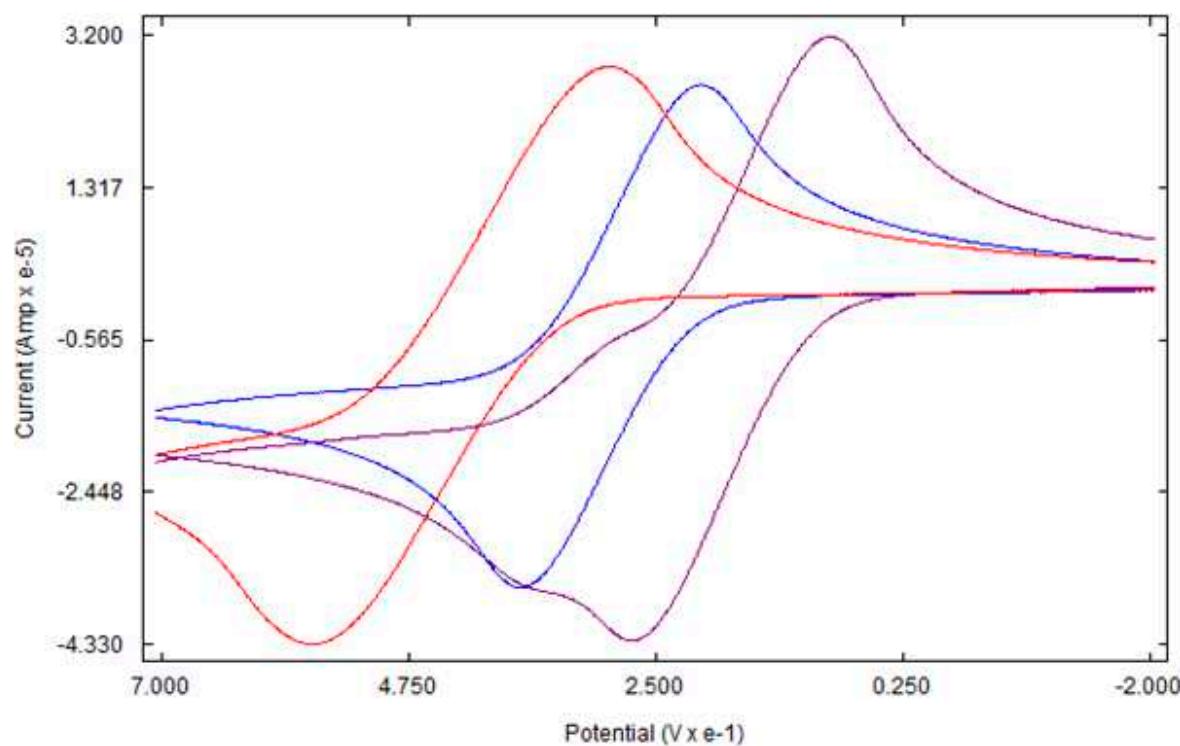
Figure 5. Cyclic voltammogram of Ferrocene (red), **4a** (blue), and **4b** (purple).

4. Conclusions.

We have synthesized and characterized mono- and bis-tetramethyleneferrocenes as viable precursors for π-extended ferrocene derivatives. Four compounds of the reaction sequence have been studied with single-crystal X-ray analysis. The effects of tetramethylene groups on the half-wave oxidation potential were studied by cyclic voltammetry. Our attempts to dehydrogenate the final products of with 2,3-dichloro-5,6-dicyano-1,4-benzoquinone (DDQ) were unsuccessful. Currently, we are working on alternative methods to aromatize the ferrocene-bound aliphatic rings.

Supplementary Materials: The following supporting information can be downloaded at the website of this paper posted on Preprints.org. Figure S1: ^{1}H NMR of **3a**; Figure S2: ^{13}C NMR of **3a**; Figure S3: IR spectrum of **3a**; Figure S4: ^{1}H NMR of **3b**; Figure S5: ^{13}C NMR of **3b**; Figure S6: IR spectrum of **3b**; Figure S7: ^{1}H NMR of **3b'**; Figure S8: ^{13}C NMR of **3b'**; Figure S9: IR spectrum of **3b'**; Figure S10: ^{1}H NMR of **4a**; Figure S11: ^{13}C NMR of **4a**; Figure S12: ^{1}H NMR of **4b**; Figure S13: ^{13}C NMR of **4b**; Figure S14: Packing diagram of **3a**; Figure S15: Packing diagram of **4a**.

Author Contributions: Conceptualization, U. P. synthesis, and spectroscopic characterization, D. D., S. N., G. E. X-ray crystallography, F. F. electrochemistry, M. L., U. P. writing – original draft preparation, U. P. writing – review and editing, U. P. and F. F. visualization, U. P. supervision, U. P. project administration, U. P. funding acquisition, U. P.

Funding: The work was funded by the Louisiana Board of Regents. Contract number: LEOSF (2017-18)-RD-A-28.

Data Availability Statement: Data are contained within the article and Supplementary materials.

Acknowledgments: The authors extend their appreciation to the Department of Chemistry and Physical Sciences, Nicholls State University for providing funds for purchasing chemicals, and the Department of Chemistry, Louisiana State University for providing X-ray crystallography services free of charge.

Preprints.org (www.preprints.org) | NOT PEER-REVIEWED | Posted: 29 January 2024 | doi:10.20944/preprints202401.0965.v2

Conflicts of Interest: The authors declare no conflict of interest.

References

1. Astruc, D. Why is ferrocene so exceptional? *European Journal of Inorganic Chemistry* **2017**, *2017*, 6-29. https://doi.org/10.1002/ejic.201600983.
2. Kealy, T.J.; Pauson, P.L. A New Type of Organo-Iron Compound. *Nature* **1951**, *168*, 1039-1040. https://doi.org/10.1038/1681039b0.
3. Yang, X.; Rominger, F.; Mastalerz, M. Benzo-Fused Perylene Oligomers with up to 13 Linearly Annulated Rings. *Angewandte Chemie International Edition* **2021**, *60*, 7941-7946, doi:org/10.1002/anie.202017062.
4. Anthony, J.E. The larger acenes: versatile organic semiconductors. *Angewandte Chemie International Edition* **2008**, *47*, 452-483, doi:org/10.1002/anie.200604045.
5. Hewison, L.; Crook, S.H.; Johnson, T.R.; Mann, B.E.; Adams, H.; Plant, S.E.; Sawle, P.; Motterlini, R. Iron indenyl carbonyl compounds: CO-releasing molecules. *Dalton Transactions* **2010**, *39*, 8967-8975. https://doi.org/10.1039/c0dt00203h.
6. Lee, S.G.; Lee, H.K.; Lee, S.S.; Chung, Y.K. Convenient Synthesis of Mixed Ferrocenes. *Organometallics* **1997**, *16*, 304-306. https://doi.org/10.1021/OM960517C.
7. Perekalin, D.S.; Babak, M.V.; Karslyan, E.E.; Nelyubina, Y.V.; Kudinov, A.R. Synthesis of iron complexes $[(\eta^5\text{-indenyl})FeL_3]^+$ from the readily available $[(\eta^5\text{-indenyl})Fe(\eta^6\text{-indene})]^+$. *Inorganica Chemica Acta* **2012**, *392*, 73-76. https://doi.org/10.1016/j.ica.2012.06.018.
8. Shirokii, V.L.; Knizhnikov, V.A.; Konovalov, T.P.; Zubreichuk, Z.P.; Erdman, A.A.; Nefedov, S.E.; Eremenko, I.L.; Yanovskii, A.I.; Struchkov, Y.T.; Maier, N.A. Electrochemical synthesis of π-indenyl-π-(3)-1,2-dicarbollyliron(III). *Izvestiya Akademi Nauk, Seriya Khimicheskaya* **1993**, 764-765.
9. Belmont, J.A.; Wrighton, M.S. Photochemical conversion of $(\eta^5\text{-}C_5H_5)Fe(CO)_2(\eta^1\text{-}C_5H_5)$ and related complexes to ferrocene and related derivatives: reactivity of the monocarbonyl intermediate. *Organometallics* **1986**, *5*, 1421. https://doi.org/10.1021/om00138a021.
10. Curnow, O.J.; Fern, G.M. Synthesis, structures and spectroelectrochemistry of methyl-substituted bis(η^5-indenyl)iron(II) complexes. *Journal of Organometallic Chemistry* **2005**, *690*, 3018-3026. https://doi.org/10.1016/j.jorganchem.2005.03.036.
11. Pokharel, U.R. Organometallic heterocycles and acene-quinone complexes of ruthenium, iron and manganese. PhD dissertation, University of Kentucky, 2012.
12. Pokharel, U.R.; Selegue, J.P.; Parkin, S. Ruthenocene 1,2-dicarboxylic acid, carboxylic anhydride, and acid chloride: A facile route to metallocene-fused acenequinones. *Organometallics* **2011**, *30*, 3254-3256. https://doi.org/10.1021/om2003915.
13. Rinehart, K.L., Jr.; Curby, R.J., Jr. Ferrocene bridging and homoannular cyclizations. *Journal of the American Chemical Society* **1957**, *79*, 3290-3291. https://doi.org/10.1021/ja01569a084.
14. Sheldrick, G. SHELXT - Integrated space-group and crystal-structure determination. *Acta Crystallographica Section A* **2015**, *71*, 3-8. https://doi.org/10.1107/S2053273314026370.
15. Sheldrick, G. Crystal structure refinement with SHELXL. *Acta Crystallographica Section C* **2015**, *71*, 3-8. https://doi.org/10.1107/S2053229614024218.
16. Patwa, A.N.; Gupta, S.; Gonnade, R.G.; Kumar, V.A.; Bhadbhade, M.M.; Ganesh, K.N. Ferrocene-linked thymine/uracil conjugates: base pairing directed self-assembly and supramolecular packing. *Journal of Organic Chemistry* **2008**, *73*, 1508-1515. https://doi.org/10.1021/jo7023416.
17. Apreutesei, D.; Lisa, G.; Hurduc, N.; Scutaru, D. Synthesis and un-isotherm kinetic study of some ferrocene acids. *Central European Journal of Chemistry* **2004**, *2*, 553-562, doi:org/10.2478/BF02482720.
18. Overbaugh, S.C.; Allen, C.F.H.; Martin, E.L.; Fieser, L.F. γ-Phenylbutyric acid. *Org. Synth.* **1935**, *XV*, 64. https://doi.org/10.15227/orgsyn.015.0064.
19. Weißenbacher, M.; Sturm, T.; Kalchhauser, H.; Kratky, C.; Weissensteiner, W. Synthesis and characterization of novel aminophosphine ligands based on ferrocenodecaline backbones. *Monatshefte für Chemie* **2002**, *133*, 991-1009. https://doi.org/10.1007/s007060200069.
20. Huffman, J.; Rabb, D. Notes- The Preparation of 1,2-(α-Ketotetramethylene)ferrocene. *The Journal of Organic Chemistry* **1961**, *26*, 3588-3589. https://doi.org/10.1021/jo01067a653.
21. Rinehart, K.L., Jr.; Curby, R.J., Jr.; Gustafson, D.H.; Harrison, K.G.; Bozak, R.E.; Bublitz, D.E. Organic chemistry of ferrocene. V. Cyclization of ω-ferrocenylaliphatic acids. *Journal of the American Chemical Society* **1962**, *84*, 3263. https://doi.org/10.1021/ja00876a010.
22. King, R.B.; Bisnette, M.B. π-Cyclopentadienyl-π-indenyliron. *Angewandte Chemie International* **1963**, *75*, 642, doi:org/10.1002/anie.196304003.
23. Bernhard, Y.; Gilbert, J.; Bousquet, T.; Favrelle-Huret, A.; Zinck, P.; Pellegrini, S.; Pelinski, L. One-Pot Synthesis of 2,5-Disubstituted Furans through In Situ Formation of Allenes and Enolization Cascade. *European Journal of Organic Chemistry* **2019**, *2019*, 7870-7873. https://doi.org/10.1002/ejoc.201901669.

24. Liu, G.; He, H.; Wang, J. Ferrocene redox controlled reversible immobilization of ruthenium carbene in ionic liquid: a versatile catalyst for ring-closing metathesis. *Advanced Synthesis & Catalysis* **2009**, *351*, 1610-1620. https://doi.org/10.1002/adsc.200800713.

25. Nesmeyanov, A.N.; Vol'kenau, N.A.; Vil'chevskaya, V.D. Intramolecular acylation in the ferrocene series. Cyclization of γ-ferrocenyl substituted acids and oxo acids. *Doklady Akademii Nauk SSSR* **1958**, *118*, 512.

26. Osiecki, J.H.; Hoffman, C.J.; Hollis, D.P. Organometallic compounds. Ruthenium and iron derivatives of indene. *Journal of Organometallic Chemistry* **1965**, *3*, 107. https://doi.org/10.1016/s0022-328x(00)84739-7.

27. Nesmeyanov, A.N.; Vol'kenau, N.A.; Vil'chevskaya, V.D. Intramolecular acylation in the ferrocene series. *Doklady Akademii Nauk SSSR* **1956**, *111*, 362-364.

28. Hallam, B.F.; Pauson, P.L. Ferrocene derivatives. IV. Indenyl- and tetrahydroindenyliron carbonyls. *Journal of the Chemical Society* **1958**, 646. https://doi.org/10.1039/jr9580000646.

29. Brandon, R.L.; Osiecki, J.H.; Ottenberg, A. Reactions of metallocenes with electron acceptors. *Journal of Organic Chemistry* **1966**, *31*, 1214. https://doi.org/10.1021/jo01342a055.

30. Fleischer, E.B.; Hawkinson, S.W. The structure of α-keto-1,5-tetramethyleneferrocene. *Acta Crystallographica* **1967**, *22*, 376-381. https://doi.org/10.1107/S0365110X67000738.

31. Schlögl, K. Stereochemistry of Metallocenes. In *Topics in Stereochemistry*; 1967; pp. 39-91.

32. Paramasivam, S.; Purushothaman, S.; Seshadri, P.R.; Raghunathan, R. (*E*)-1-Ferrocenyl-3-[2-(2-hydroxyethoxy)phenyl]prop-2-en-1-one. *Acta Crystallographica Section E* **2013**, *69*, m144. https://doi.org/10.1107/S1600536813003395.

33. Zhang, J.; Yan, S.; He, Z.; Xu, L.; Huang, S. 2-Amino-4-(4-chlorophenyl)-6-ferrocenylpyridine-3-carbonitrile. *Acta Crystallographica Section E* **2008**, *64*, m730. https://doi.org/10.1107/S1600536808008714.

34. Bratych, N.; Hassall, K.; White, J. Redetermination of the structure of diferrocenyl ketone at low temperature. *Acta Crystallographica Section E* **2003**, *59*, m33-m35. https://doi.org/10.1107/S1600536802022262.

35. Erben, M.; Ruzicka, A.; Vinklarek, J.; Stava, V.; Handlir, K. 1'-Acetylferrocene-1-carbonitrile. *Acta Crystallographica Section E* **2007**, *63*, m2145-m2146. https://doi.org/10.1107/S1600536807033892.

36. Erben, M.; Vinklarek, J.; Ruzicka, A. Acetylferrocene-2-chloro-1-ferrocenylethanone (1/1). *Acta Crystallographica Section E* **2011**, *67*, m1447-m1448. https://doi.org/10.1107/S1600536811038244.

37. Cremer, D.T.; Pople, J. General definition of ring puckering coordinates. *Journal of the American Chemical Society* **1975**, *97*, 1354-1358, doi:org/10.1021/ja00839a011.

38. Okuda, J.; Albach, R.W.; Herdtweck, E.; Wagner, F.E. Substituent effects in multiply trimethylsilyl-substituted ferrocenes. Molecular structure of 1,1',2,2',4,4'-hexakis(trimethylsilyl)ferrocenium tetrafluoroborate. *Polyhedron* **1991**, *10*, 1741-1748, doi:org/10.1016/S0277-5387(00)83794-8.

39. Tateaki, O.; Kazuo, O.; Tadashi, F.; Shunsuke, M.; Taeko, I.; Akira, K.; Nobuyuki, T. Electrochemical properties of ferrocenophanes. I. Voltammetric studies on the oxidation of mono-, di-, and tri-bridged ferrocenophanes in acetonitrile. *Bulletin of the Chemical Society of Japan* **1981**, *54*, 3723-3726. https://doi.org/10.1246/bcsj.54.3723.

40. Kuwana, T.; Bublitz, D.E.; Hoh, G. Chronopotentiometric Studies on the Oxidation of Ferrocene, Ruthenocene, Osmocene and Some of their Derivatives. *Journal of the American Chemical Society* **1960**, *82*, 5811-5817. https://doi.org/10.1021/ja01507a011.